IOPscience iopscience.iop.org

Home Search Collections Journals About Contact us My IOPscience

Eigenfunctions of non-integrable systems in generalised phase spaces

This article has been downloaded from IOPscience. Please scroll down to see the full text article.

1990 J. Phys. A: Math. Gen. 23 1745

(http://iopscience.iop.org/0305-4470/23/10/016)

View the table of contents for this issue, or go to the journal homepage for more

Download details:
IP Address: 129.252.86.83
The article was downloaded on 31/05/2010 at 15:04

Please note that terms and conditions apply.

J. Phys. A: Math. Gen. **23** (1990) 1745–1764. Printed in the UK

Eigenfunctions of non-integrable systems in generalised phase spaces

P Leboeuf† and M Saraceno

Departamento de Física, Comisión Nacional de Energía Atómica, 1429 Buenos Aires, Argentina and Institute for Theoretical Physics, University of California, Santa Barbara, California 93106, USA

Received 13 November 1989, in final form 29 January 1990

Abstract. We use the generalised coherent state distribution to study in phase space the eigenfunctions of non-integrable Hamiltonians. The methods available in the Weyl group (the Husimi distribution) are extended to the more complicated phase spaces that arise from other Lie groups. We demonstrate the feasibility of numerical calculations in two models with W_2 and SU(3) symmetries, emphasising the similarities and showing the emergence of classical invariant structures in the semiclassical limit.

1. Introduction

The understanding of the classical–quantum correspondence for non-integrable systems is a subject of considerable current interest which still has wide gaps. In particular, the way in which a wavepacket, following a classical trajectory by way of Ehrenfest's theorem, spreads and interferes with itself when this trajectory is chaotic to finally produce as $t \to \infty$ a stationary eigenstate is not understood. There is no Bohr–Sommerfeld quantisation rule for non-integrable systems [1].

In recent years most efforts devoted to the study of the quantum properties of classically chaotic systems were focused on the statistical properties of the spectrum [2–4], and methods to relate these properties to the periodic orbit structure have been devised [5–9]. Wavefunctions, however, provide a richer context for the study of the correspondence principle since we expect the invariant structures of classical mechanics to be reflected in the stationary states of quantum mechanics.

For integrable systems it is well known that eigenfunctions are associated with the quantised invariant tori. The actions of these tori provide a complete set of quantum numbers through the EBK quantisation rules.

In the non-integrable case the situation is far more complex. The phase space contains an intricate mixture of stable and unstable periodic trajectories, tori, cantori and chaotic regions. No simple association between these structures and stationary states is known.

For the chaotic regions the simple hypothesis of a uniform, ergodic-like distribution—the celebrated hypothesis of Berry and Voros [1]—breaks down due

† Present address: Division de Physique Théorique, Institut de Physique Nucléaire, 91406 Orsay Cedex, France.

0305-4470/90/101745+20$03.50 © 1990 IOP Publishing Ltd

to the presence of unstable periodic trajectories [10, 11] and cantori [12–15]. Both structures, although classically of measure zero on the energy shell, have a dominant influence on the wavefunctions and result in a completely different quantum and classical long-time behaviour. Based on the periodic orbit sum of Gutzwiller [16], recent studies [17–20] have begun to provide a theoretical understanding of the role played by unstable periodic trajectories and the associated homoclinic motion [19].

These problems are usually considered in the framework of the $\hbar \to 0$ limit of quantum mechanics. However, a wider class of semiclassical limits arises in connection to $1/N$ expansions (see [21] and references therein). Their main difference with the $\hbar \to 0$ limit is the structure of the phase space. In the usual case the underlying group is the Weyl group which leads to a 'flat' phase space. For other groups the semiclassical limit leads to phase spaces with a more complicated structure which corresponds to the coadjoint orbits of the group. The problem of recovering quantum properties of such systems from its $N \to \infty$ limit are exactly those encountered in semiclassical mechanics and the issues related to chaotic behaviour will have to be addressed.

The purpose of this paper is to develop the methods that allow the study of wavefunctions in these generalised phase spaces. We use coherent states of Lie groups [22] to represent the eigenstates as a positive definite phase space distribution and study numerically the associated projections and Poincaré sections. To keep the classical dynamics as manageable as possible we restrict our considerations to phase spaces of dimension four with a conserved Hamiltonian.

The outline of the paper is as follows. In section 2, after a brief survey of the Husimi distribution for the group W_1, we generalise it for semisimple Lie groups and show how to calculate its projections and Poincaré sections. In section 3 we study the specific examples of W_2 and SU(3) and we emphasise the similarity between the two cases. W_2 is of course the group underlying the treatment of coupled oscillator models, while SU(3) is more related to model nuclear Hamiltonians with interacting fermions. The parallel treatment aims at stressing the fact that methods used for the study of chaos in one of them can be also used in the other. In section 4 we present a collection of numerical results and discussion for the wavefunctions, projections and sections for two models with these symmetries.

2. Phase space representation of eigenfunctions

2.1. The simple case of the Weyl W_1 group

In this section we review some basic properties of W_1 coherent states and the associated distributions in phase space.

For a system with one degree of freedom, we define

$$\hat{a}^+ = \frac{1}{\hbar\sqrt{2}} \left(\hat{q}/b_0 - \mathrm{i}b_0\hat{p}\right) \tag{2.1}$$

and the coherent state

$$|z\rangle = \exp(\bar{z}\hat{a}^+)|0\rangle \tag{2.2}$$

where $a|0\rangle = 0$ and z is a complex number and $\bar{z}$ its conjugate. The parameter b_0 characterises the width of the localised wavepacket $|z\rangle$ while the real and imaginary

parts of z are related to the classical phase space coordinates (p, q) by

$$z = \frac{1}{\sqrt{2}} (q/b_0 - \mathrm{i}b_0 p) \tag{2.3}$$

and thus coordinates $(z, \bar{z})$ span the canonical phase space. The Husimi distribution [23] of a given state $|\psi\rangle$ is defined as

$$W_\psi(p, q) = \frac{|\langle z|\psi\rangle|^2}{\langle z|z\rangle} \tag{2.4}$$

where the norm is

$$\langle z|z\rangle = \exp\left(\frac{z\bar{z}}{\hbar}\right). \tag{2.5}$$

The coherent state $|z\rangle$ is a Gaussian wavepacket centred at the phase space point (p, q) and with dispersions

$$\Delta^2\hat{q} = \frac{b_0^2\hbar}{2} \qquad \Delta^2\hat{p} = \frac{\hbar}{2b_0^2}. \tag{2.6}$$

Therefore, (2.4) gives the probability for the wavefunction ψ to be in the phase space cell $\Delta q \Delta p$ centred at (p, q), compatible with the uncertainty principle requirements.

There is a different way to represent a state in phase space: the Wigner distribution [24, 25]. It is defined as

$$\mathscr{W}_\psi(p, q) = \frac{1}{2\pi\hbar} \int \mathrm{d}x \, \langle x - q/2|\psi\rangle\langle\psi|x + q/2\rangle \mathrm{e}^{\mathrm{i}xp/\hbar} \tag{2.7}$$

and carries in phase space all the quantum information associated with the density matrix $\rho(x, x')$. The relationship of the Wigner and Husimi distributions is given by

$$W_\psi(p, q) = \int \mathrm{d}p' \, \mathrm{d}q' \, Z_{p'q'}(p, q) \mathscr{W}_\psi(p, q) \tag{2.8}$$

where

$$Z_{p'q'}(p, q) = \frac{1}{\pi\hbar} \exp\left\{-\frac{(q - q')^2}{\hbar b_0^2} - b_0^2 \frac{(p - p')^2}{\hbar}\right\} \tag{2.9}$$

is the Wigner distribution of the normalised coherent state $|z\rangle/\sqrt{\langle z|z\rangle}$. The Husimi distribution of a state $|\psi\rangle$ is thus obtained by smoothing its Wigner distribution with a Gaussian. From (2.9) we see that by changing b_0 we can change the width of the smoothing in the p and q directions while maintaining $\Delta q \Delta p$ constant. On the contrary, letting $\hbar \to 0$ sharpens both scales at once.

According to its definition (2.4), the Husimi distribution is a positive definite function in phase space. For systems with one degree of freedom with a conserved Hamiltonian the Husimi distribution of an eigenstate ψ_i of energy E_i can be shown [26] to be localised on the constant energy contour E_i according to the semiclassical formula

$$W_{\psi_i}(z, \bar{z}) \approx \frac{c}{v(z, \bar{z})} \exp\left[-\frac{2}{\hbar}\left(\frac{H_{\mathrm{cl}}(z, \bar{z}) - E_i}{v(z, \bar{z})}\right)^2\right] \tag{2.10}$$

where $v(z,\bar{z})$ is the modulus of the phase space velocity $v = |\partial H_{cl}/\partial z|$, H_{cl} is the classical Hamiltonian and c is a normalisation. This formula has been further discussed and generalised to the groups SU(2) and SU(1,1) in [27].

This simple Gaussian peaking on the classical trajectory should be contrasted with that of the semiclassical Wigner function, studied by Berry [28], which shows Airy-type behaviour on the tori, sharp oscillations on the inside and an exponential decay on the outside.

This difference is clearly illustrated when we consider the distribution of a pure oscillator state $|n\rangle$. Then (2.4) yields

$$W_n(z,\bar{z}) = \frac{(z\bar{z}/\hbar)^n \, e^{-z\bar{z}/\hbar}}{n!}. \tag{2.11}$$

This is a Poisson distribution with its maximum at $z\bar{z}/\hbar = n$. For large values of n, this maximum becomes very sharp, with a width $\sqrt{n}$. The Wigner distribution of the oscillator state is given instead by

$$\mathcal{W}_n(z,\bar{z}) = (-1)^n \, e^{-2z\bar{z}/\hbar} \, L_n(4z\bar{z}/\hbar) \tag{2.12}$$

where L_n are the Laguerre polynomials. It has very strong oscillations and takes positive and negative values. Although it has a relative maximum close to the classical trajectory $z\bar{z}/\hbar = n$, it assumes its largest value at the origin, where nothing happens classically.

2.2. Husimi distributions for general Lie groups

The simple Husimi distribution defined in the previous section corresponds to the coherent states of the Weyl group W_1. One immediate generalisation is the extension to the W_n group which allows the treatment of systems with many independent degrees of freedom spanned by canonical pairs (p_i, q_i).

Other extensions more appropriate for the treatment of many-body or finite spin systems occur when the Hamiltonian can be written in terms of the generators of a Lie group G. In this case the semiclassical limit is obtained as some parameter of the group representation N, which can be identified in each case, goes to infinity. The classical phase space that arises from this procedure is a symplectic manifold whose geometrical properties are characteristic of the group [29]. In particular it has a finite volume for compact groups. We now provide the essential steps of this construction [22].

For semisimple groups the canonical form of the commutation relations allow the splitting of the algebra $\mathcal{L}$ into raising, lowering and weight operators, (E^+, E^-, H). For our purposes, the coherent states of a given representation are conveniently defined as

$$|\mathbf{z}\rangle = \exp\left(\sum_i \bar{z}_i E_i^+\right)|0\rangle \tag{2.13}$$

where E_i^+ are the raising operators in the algebra and $|0\rangle$ is the minimum weight state of an irreducible representation of G characterised by

$$\begin{aligned} H_\alpha|0\rangle &= h_\alpha|0\rangle \\ E_i^-|0\rangle &= 0. \end{aligned} \tag{2.14}$$

H_α are the commuting weight operators spanning the Cartan (or isotropy) subalgebra of $\mathscr{L}$. The coordinates z span a manifold $\mathscr{M}$ which has the following important properties:

(i) there is a one-to-one correspondence between $\mathscr{M}$ and the set of points generated by the action of the coadjoint representation of the group (the so-called coadjoint orbit);

(ii) it can be shown that coadjoint orbits of nilpotent and compact semisimple Lie groups are real manifolds of even dimension having a closed non-degenerate (G-invariant) two-form, i.e, they are symplectic manifolds.

Hence the set of coherent states are parametrised by points of a space $\mathscr{M}$ which can be considered as a generalised version of the canonical phase space for Hamiltonians written in terms of the generators of a given Lie group G.

All the geometrical quantities on $\mathscr{M}$ are related to the norm function $\langle z|z\rangle$ which can be explicitly evaluated for each representation. The antisymmetric non-degenerate two-form Ω is defined as

$$\Omega = 2\mathrm{i}\omega^{ij}\mathrm{d}z_i \wedge \mathrm{d}\bar{z}_j \tag{2.15}$$

where

$$\omega^{ij} = \frac{1}{N}\frac{\partial^2}{\partial z_i \partial \bar{z}_j}\ln\langle z|z\rangle. \tag{2.16}$$

The generalised Poisson bracket on $\mathscr{M}$ is

$$\{f, g\} = \mathrm{i}\omega_{ij}\left(\frac{\partial f}{\partial z_i}\frac{\partial g}{\partial \bar{z}_j} - \frac{\partial f}{\partial \bar{z}_i}\frac{\partial g}{\partial z_j}\right) \tag{2.17}$$

where ω_{ij} is the inverse matrix of ω^{ij}.

A basis of an irreducible representation can be generated, as is well known, by repeated action of the raising generators on the minimum weight state. This basis is appropriate for quantum mechanical calculations if a Hamiltonian is given as a function of the generators of G. Coherent states provide an alternative representation [30]. In this representation, the wavefunction

$$\psi(z) = \langle z|\psi\rangle \tag{2.18}$$

is given by an analytic function of the coset coordinates $\{z\}$. The operators can be represented either by functions on $\mathscr{M}$ as

$$A(z, \bar{z}) = \frac{\langle z|\hat{A}|z\rangle}{\langle z|z\rangle} \tag{2.19}$$

or by differential operators acting on (2.18). The important feature of this representation is the fact that it allows a very straightforward emergence of the classical limit. This is based on the following property [21]

$$\frac{\langle z|\hat{A}\hat{B}|z\rangle}{\langle z|z\rangle} = AB + \frac{1}{N}\,\omega_{ij}\frac{\partial A}{\partial z_i}\frac{\partial B}{\partial \bar{z}_j} + \ldots \tag{2.20}$$

which shows that, to order zero in $1/N$ the product of operators factors. The $1/N$ correction in (2.20) determines the limit for commutators as

$$\lim_{N\to\infty} \frac{N}{\mathrm{i}} \frac{\langle z|[\hat{A},\hat{B}]|z\rangle}{\langle z|z\rangle} = \{A_{\mathrm{cl}}, B_{\mathrm{cl}}\} \tag{2.21}$$

where the bracket is the symplectic structure (2.17) on $\mathcal{M}$.

Using equation (2.21), the Heisenberg equation for operators has the limit

$$\frac{\mathrm{d}A_{\mathrm{cl}}}{\mathrm{d}t} = \{A_{\mathrm{cl}}, H_{\mathrm{cl}}\}. \tag{2.22}$$

The classical symbol used in (2.21) and (2.22) is defined by

$$A_{\mathrm{cl}}(z,\bar{z}) = \lim_{N\to\infty} A(z,\bar{z}). \tag{2.23}$$

The Hamiltonian H_{cl}, which describes this limiting behaviour, is obtained as in (2.23). The behaviour of eigenstates in this limit constitutes the central theme of our study. The objective is to correlate the invariant structures arising in the classical limit with the stationary states ψ. For this purpose, we use the generalised Husimi distribution

$$W_\psi(z,\bar{z}) = \frac{\langle z|\psi\rangle\langle\psi|z\rangle}{\langle z|z\rangle} \tag{2.24}$$

which is just (2.19) for the density operator. This definition associates with each wavefunction a distribution on $\mathcal{M}$ with the following properties:

(i) $$1 \geq W_\psi(z,\bar{z}) \geq 0. \tag{2.25}$$

The first inequality follows from Schwartz' inequality applied to (2.24).

(ii) $$\int_{\mathcal{M}} \mathrm{d}\mu(z)\, W_\psi(z,\bar{z}) = 1, \tag{2.26}$$

where $\mathrm{d}\mu(z)$ is the invariant measure on $\mathcal{M}$. $\mathrm{d}\mu(z)$ depends on the group (i.e., on the geometry of $\mathcal{M}$) and sets the normalisation of W_ψ with respect to its limiting behaviour towards the classical distribution. For example, it is $(1/\pi\hbar)\mathrm{d}^2z$ for the Weyl W_1 group and $[(2j+1)/\pi](\mathrm{d}^2z/(1+z\bar{z})^2)$ for the SU(2) group, where j is the spin quantum number. Equation (2.25) together with (2.26) suggest that W_ψ can be interpreted as a probability distribution. It represents the probability of observing the state in $|z\rangle$ which is a narrow phase space packet on $\mathcal{M}$ (however, some care must be taken in this interpretation due to the non-orthogonality of the coherent states).

(iii) Energy localisation. Using (2.20) we can write approximately the Schrödinger equation $\hat{H}\hat{\rho} = E\hat{\rho}$ as

$$(H_{\mathrm{cl}}(z,\bar{z}) - E)\, W_\psi = \frac{1}{N}\, \omega_{ij} \frac{\partial H_{\mathrm{cl}}}{\partial z_i} \frac{\partial W_\psi}{\partial \bar{z}_j} + \mathrm{O}\left(\frac{1}{N^2}\right). \tag{2.27}$$

To order zero in $1/N$ the solution of this equation is

$$W_\psi^{(0)} \simeq \delta(H_{\rm cl}(z,\bar{z}) - E)F(z,\bar{z}) \tag{2.28}$$

that is, a delta function peaked on the quantised energy E. The function $F(z,\bar{z})$ provides all the interesting information about the distribution on the energy shell that does not follow directly from energy conservation. If we include the next order $(1/N)$ the delta function is smoothed [26, 27] to a Gaussian peaked at the classical energy surface $H_{\rm cl}(z,\bar{z}) = E$.

(iv) If other quantum constants of the motion $\hat{A}_i$ exist such that $[\hat{H},\hat{A}_i] = [\hat{A}_i,\hat{A}_j] = 0$, then the same argument shows that W_ψ localises on each of the classical surfaces $A_i(z,\bar{z}) = a_i$. If there are enough of these to make the classical motion integrable, then W_ψ will be peaked on the invariant tori. In the general case of a classically non integrable system, the general structure of $F(z,\bar{z})$ is not known.

The outcome of this procedure is then a mapping of an irreducible unitary representation of a Lie group into a classical phase space. This mapping has been called dequantisation and studied in the context of the time-dependent variational principle [31]. It is the inverse procedure of the much more difficult problem of geometric quantisation [32], i.e. the finding of unitary irreducible representations associated with general symplectic manifolds.

2.3. Poincaré sections of quantum eigenstates

As we show below, generalised Husimi distributions for eigenstates of time-independent Hamiltonians with two degrees of freedom are easily calculated. However, they are four-dimensional objects whose visualisation and graphical display are difficult. Just as in the classical counterpart, we circumvent this difficulty by defining projections and Poincaré sections of the quantum distributions defined on $\mathcal{M}$. Classically, a Poincaré map for a conservative system is defined by eliminating one variable on account of energy conservation and taking a fixed value for its canonical conjugate [33]. The dimension of phase space is lowered by two and time is eliminated completely while the sections are labelled by the energy. Quantum mechanically, we obtain a construction comparable to the above procedure by integrating a stationary distribution over one variable and fixing another one, which defines the plane of section. Thus, for example

$$S_{q_2}(p_1,q_1) = \int \mathrm{d}p_2\, W_\psi(p_1,q_1,p_2,q_2) \tag{2.29}$$

defines a probability distribution in the variables (p_1,q_1) obtained in the section plane q_2. Other sections are defined in a similar fashion. In (2.29) we are using canonical coordinates $(\boldsymbol{p},\boldsymbol{q})$ which can always be defined from $(z,\bar{z})$ because of Darboux theorem [29]. An alternative definition is to restrict the distribution to the energy surface, i.e. define instead of (2.29)

$$S'_{q_2}(p_1,q_1) = W_\psi(p_1,q_1,p_2(E,p_1,q_1,q_2),q_2) \tag{2.30}$$

where E is the energy of the eigenstate $|\psi\rangle$ and $p_2(E,p_1,q_1,q_2)$ is obtained from the classical Hamiltonian. This is the definition used in references [34] and [35] to study the wavefunctions of oscillator systems in the Husimi or Wigner representation. Because the distribution in the semiclassical limit is sharply peaked on the energy shell, the

integration in (2.29) effectively picks up only contributions very close to it and the result of both definitions essentially coincide.

Projections are obtained by integrating over two variables, i.e.

$$P(q_1, q_2) = \int \mathrm{d}p_1 \, \mathrm{d}p_2 \, W_\psi(p_1, q_1, p_2, q_2) \tag{2.31}$$

which projects the distribution on the plane (q_1, q_2) and provides a smoothed version of the wavefunction probability $|\psi(q_1, q_2)|^2$.

3. W_2 and SU(3) coherent states in action–angle variables

3.1. Coupled harmonic oscillator models. The group W_2

In this section we consider two-dimensional conservative systems whose Hamiltonian is written in terms of the W_2 algebra

$$\begin{aligned} &[\hat{q}_i, \hat{p}_j] = \mathrm{i}\hbar\delta_{ij} \, \boldsymbol{I} \\ &\qquad\qquad\qquad\qquad i, j = 1, 2 \\ &[\hat{q}_i, \hat{q}_j] = [\hat{p}_i, \hat{p}_j] = 0. \end{aligned} \tag{3.1}$$

We illustrate in this well known case the general procedure described in section 2.2.

The raising operators

$$a_i^+ = \frac{1}{\hbar\sqrt{2}} \left(\hat{q}_i / b_i - \mathrm{i} b_i \hat{p}_i\right) \tag{3.2}$$

are used to define the coherent states

$$|z_1 z_2\rangle = \exp(\bar{z}_1 a_1^+ + \bar{z}_2 a_2^+) \, |0\rangle \tag{3.3}$$

where $a_i|0\rangle = 0$ and the parameters b_i define the frequency of the oscillator basis.

The coadjoint orbits spanned by parameters (z_1, z_2) are simply four-dimensional planes and for a given value of $\hbar$ coincide with the classical phase space. The $(\boldsymbol{p}, \boldsymbol{q})$ coordinates are related to $(\boldsymbol{z}, \bar{\boldsymbol{z}})$ by

$$z_i = \frac{1}{\sqrt{2}} \left(q_i / b_i - \mathrm{i} b_i p_i\right). \tag{3.4}$$

In the classical limit the Hamiltonian is

$$H_{\mathrm{cl}}(\boldsymbol{z}, \bar{\boldsymbol{z}}) = \lim_{\hbar \to 0} \frac{\langle z_1 z_2 | \hat{H} | z_1 z_2 \rangle}{\langle z_1 z_2 | z_1 z_2 \rangle} \tag{3.5}$$

while the norm function that determines the structure of the phase space is

$$\langle z_1 z_2 | z_1 z_2 \rangle = \exp\left\{ \frac{1}{\hbar} (z_1 \bar{z}_1 + z_2 \bar{z}_2) \right\}. \tag{3.6}$$

The calculation of $\langle z_1 z_2 | \psi \rangle$ is very simple when $|\psi\rangle$ is known in the oscillator basis

$$|n_1 n_2\rangle = \sqrt{\frac{\hbar^{n_1} \hbar^{n_2}}{n_1 ! n_2 !}} \, (a_1^+)^{n_1} (a_2^+)^{n_2} \, |0\rangle. \tag{3.7}$$

In fact, from (3.3) and (3.7) we can write

$$|z_1 z_2\rangle = \sum_{n_1,n_2=0}^{\infty} \sqrt{\frac{1}{\hbar^{n_1}\hbar^{n_2} n_1!\, n_2!}}\,(\bar{z}_1)^{n_1}(\bar{z}_2)^{n_2}\,|n_1 n_2\rangle \tag{3.8}$$

by means of which the Husimi distribution (2.24) can be expressed as

$$\begin{aligned} W_\psi(z_1,\bar{z}_1,z_2,\bar{z}_2) &= \frac{|\langle z_1 z_2|\psi\rangle|^2}{\langle z_1 z_2|z_1 z_2\rangle} \\ &= \left|\sum_{n_1 n_2=0}^{\infty} \langle z_1 z_2|n_1 n_2\rangle\langle n_1 n_2|\psi\rangle\right|^2 \langle z_1 z_2|z_1 z_2\rangle^{-1} \\ &= \left|\sum_{n_1 n_2=0}^{\infty} \sqrt{\frac{\exp[-(z_1\bar{z}_1+z_2\bar{z}_2)/\hbar]}{\hbar^{n_1} n_1!\hbar^{n_2} n_2!}}\; z_1^{n_1} z_2^{n_2}\,\langle n_1 n_2|\psi\rangle\right|^2 . \end{aligned} \tag{3.9}$$

In this context it is convenient to introduce the action–angle variables of the oscillators

$$z_i = \sqrt{I_i}\,\mathrm{e}^{\mathrm{i}\theta_i} \tag{3.10}$$

which allows us to rewrite (3.9) as

$$\begin{aligned} &W_\psi(I_1,\theta_1,I_2,\theta_2) \\ &\quad = \left|\sum_{n_1,n_2=0}^{\infty} \sqrt{\frac{\mathrm{e}^{-I_1/\hbar}\,(I_1/\hbar)^{n_1}}{n_1!}}\sqrt{\frac{\mathrm{e}^{-I_2/\hbar}\,(I_2/\hbar)^{n_2}}{n_2!}}\,\exp[\mathrm{i}(n_1\theta_1+n_2\theta_2)]\langle n_1 n_2|\psi\rangle\right|^2 . \end{aligned} \tag{3.11}$$

It is worthwhile to analyse the structure of (3.11) because it recurs for all other groups. The wavefunction $|n_1\ n_2\rangle$ can be thought of as having sharply defined (and discrete) values of the actions $\hbar n_1$ and $\hbar n_2$. Therefore the conjugate variables θ_i are completely delocalised. To obtain a wavepacket localised both in action and angle (and therefore localised at a point (I_i,θ_i) in phase space where we are calculating the distribution) we need to take a narrow superposition of different states $|n_1\ n_2\rangle$ and add the appropriate phase $\exp(\mathrm{i}n_i\theta_i)$, as in (3.11). The structure of this equation will be valid for more general semisimple Lie groups. What changes from group to group is the exact shape of the wavepacket, i.e., the prefactors contained in the square roots. In the present case of the W_2 group, the smoothing of the $\langle n_1 n_2|\psi\rangle$ wavefunction is Poisson, as pertains to variables bounded from below (both $I_i \geq 0$ and $n_i \geq 0$). This is seen more clearly if we integrate over the angles to obtain the projection in action variables (cf equation (2.31))

$$\begin{aligned} P(I_1,I_2) &= \int_0^{2\pi} \mathrm{d}\theta_1\,\mathrm{d}\theta_2\, W_\psi(I_1,\theta_1,i_2,\theta_2) \\ &= 4\pi^2 \sum_{n_1,n_2=0}^{\infty} \frac{\mathrm{e}^{-I_1/\hbar}\,(I_1/\hbar)^{n_1}}{n_1!}\,\frac{\mathrm{e}^{-I_2/\hbar}\,(I_2/\hbar)^{n_2}}{n_2!}\,|\langle n_1 n_2|\psi\rangle|^2 . \end{aligned} \tag{3.12}$$

The projection of the distribution in terms of the continuous classical action variables I_i is thus obtained by a Poisson smoothing of the discrete wavefunction probability $|\langle n_1 n_2|\psi\rangle|^2$. This smoothing will reveal more and more details of the classical structures as $\hbar \to 0$. For large quantum numbers the Poisson distribution approximates a gaussian centred at $I_i = \hbar n_i$ and with a dispersion proportional to $\sqrt{n_i}$. Thus the smoothing, while becoming infinitely sharp, will always involve many components of the wavefunction.

In these variables, several planes of section can be used. Close to the integrable system described by the quantised tori (n_1, n_2), the more useful sections would be θ-sections obtained by integrating over an action, say I_2, and fixing the conjugate angle, say to $\theta_2 = 0$. These sections would then be (cf equation (2.29))

$$S_{\theta_2=0}(I_1, \theta_1) = \int \mathrm{d}I_2 \, W_\psi(I_1, \theta_1, I_2, \theta_2 = 0). \tag{3.14}$$

However, when studying Hamiltonians very far from the integrable limit it does not matter which sections one considers and the I-sections are much more economical to compute. The reason is that the θ integral can be done analytically and reduces by one the sums in (3.11). For I-sections we compute the distribution as

$$\begin{aligned} S_{I_2}(I_1, \theta_1) &= \int_0^{2\pi} \mathrm{d}\theta_2 \, W_\psi(I_1, \theta_1, I_2, \theta_2) \\ &= 2\pi \sum_{n_2=0}^{\infty} \frac{\mathrm{e}^{-I_2/\hbar} (I_2/\hbar)^{n_2}}{n_2!} \left| \sum_{n_1=0}^{\infty} \sqrt{\frac{\mathrm{e}^{-I_1/\hbar} (I_1/\hbar)}{n_1!}} \mathrm{e}^{\mathrm{i}n_1\theta_1} \langle n_1 n_2|\psi\rangle \right|^2 . \end{aligned} \tag{3.15}$$

3.2. SU(3) models

We are interested here in Hamiltonians which are written in terms of the nine generators $(G_{ij}, i, j = 0, 1, 2)$ of the U(3) group

$$[G_{ij}, G_{kl}] = \delta_{jk} G_{il} - \delta_{il} G_{kj} \qquad (i, j = 0, 1, 2). \tag{3.16}$$

We will only discuss the $[N, 0, 0]$ irreducible representation of the group and follow here the standard notation for the unitary group used by Moshinsky [36]. The representation $[N, 0, 0]$ is characterised by a minimum weight state $|0\rangle$ satisfying the conditions $G_{11}|0\rangle = N|0\rangle$, $G_{22}|0\rangle = G_{33}|0\rangle = 0$ and $G_{12}|0\rangle = G_{13}|0\rangle = G_{23}|0\rangle = 0$. The constraint $G_{00} + G_{11} + G_{22} = N$ reduces the algebra to an SU(3) group.

According to the general scheme described in section 2.2, we obtain the coherent states of this group applying the exponentials of the raising generators G_{10}, G_{20}, G_{21} to the minimum weight state of the representation. For the $[N, 0, 0]$ representation the action of G_{21} is trivial and the generic six-dimensional coadjoint orbits of SU(3) reduce to simpler four-dimensional manifolds [31]. The coherent states for $[N, 0, 0]$ are therefore defined as

$$|z_1 z_2\rangle = \exp(\bar{z}_1 G_{10} + \bar{z}_2 G_{20})\,|0\rangle \tag{3.17}$$

whose norm is

$$\langle z_1 z_2|z_1 z_2\rangle = (1 + z_1\bar{z}_1 + z_2\bar{z}_2)^N. \tag{3.18}$$

For this representation, quantum mechanics occurs in a finite-dimensional Hilbert space whose basis can be labelled by two integers

$$|n_1 n_2\rangle = \sqrt{\frac{(N-n_1-n_2)!}{N!n_1!n_2!}}\, G_{10}^{n_1} G_{20}^{n_2} |0\rangle \tag{3.19}$$

where $0 \le n_1 + n_2 \le N$. In terms of this basis the coherent states are given by

$$|z_1, z_2\rangle = \sum_{\substack{n_1,n_2=0 \\ n_1+n_2\le N}}^{N} \left[\frac{N!}{n_1!n_2!(N-n_1-n_2)!}\right]^{1/2} \bar{z}_1^{n_1} \bar{z}_2^{n_2} |n_1 n_2\rangle. \tag{3.20}$$

The symplectic structure is derived from (3.18) using the inverse of matrix (2.16)

$$\omega_{ij} = (\omega^{ij})^{-1} = (1 + z_1\bar{z}_1 + z_2\bar{z}_2) \begin{pmatrix} 1+z_1\bar{z}_1 & z_2\bar{z}_1 \\ z_1\bar{z}_2 & 1+z_2\bar{z}_2 \end{pmatrix}. \tag{3.21}$$

This structure can be transformed to canonical form through the following transformation

$$z_j = \sqrt{\frac{I_j}{1-I_1-I_2}}\, e^{i\theta j} \qquad j = 1, 2. \tag{3.22}$$

The significance of the I_j is easy to establish: they are the classical functions associated with the weight operators G_{jj}

$$I_j = \frac{1}{N}\frac{\langle z_1 z_2|G_{jj}|z_1 z_2\rangle}{\langle z_1 z_2|z_1 z_2\rangle} = \frac{z_j\bar{z}_j}{1+z_1\bar{z}_1+z_2\bar{z}_2}. \tag{3.23}$$

satisfying the following boundary conditions

$$\begin{aligned} &0 \le I_j \le 1 \\ &0 \le I_1 + I_2 \le 1 \end{aligned} \tag{3.24}$$

as follows from (3.23).

The phase space is therefore of finite volume, which is a reflection of the compactness of the group. The classical limit is obtained for $N \to \infty$ in which the discrete quantum numbers $(n_1/N, n_2/N)$ become the continuous action variables (I_1, I_2). Therefore this limit can be thought of as an asymptotic property of the eigenvalues and eigenfunctions of a sequence of large finite matrices, without any truncations involved. This will be a general feature of compact groups.

Using equations (3.18), (3.20) and definition (2.24), the Husimi distribution written in terms of the (I_i, θ_i) variables takes the form

$$\begin{aligned} &W_\psi(I_1, \theta_1, I_2, \theta_2) \\ &= \left| \sum_{\substack{n_1,n_2=0 \\ n_1+n_2\le N}}^{N} \left[\frac{N!}{n_1!n_2!(N-n_1-n_2)!} I_1^{n_1} I_2^{n_2} (1-I_1-I_2)^{N-n_1-n_2}\right]^{1/2} \right. \\ &\qquad \left. \times \exp[i(n_1\theta_1 + n_2\theta_2)]\langle n_1 n_2|\psi\rangle \right|^2. \end{aligned} \tag{3.25}$$

Projecting the Husimi distribution in the $I_1 I_2$ plane we obtain

$$P(I_1, I_2) = \int_0^{2\pi} d\theta_1 \, d\theta_2 \, W_\psi(I_1, \theta_1, I_2, \theta_2)$$

$$= 4\pi^2 \sum_{\substack{n_1, n_2 = 0 \\ n_1 + n_2 \leq N}}^{N} \frac{N!}{n_1! n_2! (N - n_1 - n_2)!} {I_1}^{n_1} {I_2}^{n_2} (1 - I_1 - I_2)^{N - n_1 - n_2} |\langle n_1 n_2 | \psi \rangle|^2. \tag{3.26}$$

The comparison of equations (3.25)–(3.26) and equations (3.11)–(3.12) is very illuminating. The finite size of the representation has resulted merely in a change of the smoothing which is now trinomial instead of Poisson. In the large N limit this difference is quite small (except near the boundaries of (3.24)). In fact both smoothings become Gaussian with a width $1/\sqrt{N}$ in this latter case.

Just as in the W_2 case, one can consider either θ or I sections. We have mainly studied the latter, which are given by

$$S_{I_2}(I_1, \theta_1) = \int d\theta_2 \, W_\psi(I_1, \theta_1, I_2, \theta_2)$$

$$= 2\pi \sum_{n_2 = 0}^{N} \frac{{I_2}^{n_2}}{n_2!} \left| \sum_{n_1 = 0}^{N - n_2} \left[\frac{N!}{n_1! (N - n_1 - n_2)!} {I_1}^{n_1} \right.\right.$$

$$\left.\left. \times (1 - I_1 - I_2)^{N - n_1 - n_2} \right]^{1/2} e^{i n_1 \theta_1} \langle n_1 n_2 | \psi \rangle \right|^2. \tag{3.27}$$

4. Numerical studies

As examples of W_2 and SU(3) systems we present here a survey of results for the eigenstates of two conservative systems with two freedoms: (a) the Nelson [37] Hamiltonian

$$\hat{H} = \frac{1}{2} (\hat{p}_x^2 + \hat{p}_y^2) + \left(\hat{y} - \frac{\hat{x}^2}{2} \right)^2 + \mu \frac{\hat{x}^2}{2} \tag{4.1}$$

and (b) the SU(3) Lipkin model [38]

$$\hat{H} = \sum_{i=0}^{2} \epsilon_i G_{ii} + \frac{1}{2} V \sum_{i \neq j} G_{ij}^2. \tag{4.2}$$

In both cases the Hamiltonian is written in terms of the generators of the associated group. The Hamiltonian (4.1) is a modified Henon–Heiles potential typical of many molecular systems. It has been used to calculate numerically the families of periodic trajectories and their bifurcations [37]. The model represented by (4.2) is characteristic of nuclear shell model structure with single particle energies ϵ_i and a simplified two-body interaction. It has been studied in connection with many body approximation

techniques and semiclassical quantisation [39] and its spectral statistics have been analysed [40] .

The classical Hamiltonians in action–angle variables are

$$H_{\mathrm{cl}}^{\mathrm{Nelson}} = \sqrt{\mu} I_1 + \sqrt{2} I_2 + \frac{1}{\mu} I_1 \cos^2\theta_1 (I_1 \cos^2\theta_1 - 2^{5/4}\sqrt{\mu I_2}\cos\theta_2) \tag{4.3}$$

and

$$H_{\mathrm{cl}}^{SU(3)} = -1 + I_1 + 2I_2 + \chi(1 - I_1 - I_2)(I_1 \cos 2\theta_1 + I_2 \cos 2\theta_2) + \chi I_1 I_2 \cos 2(\theta_2 - \theta_1). \tag{4.4}$$

They were obtained as (cf equation (2.23))

$$H_{\mathrm{cl}} = \lim_{\lambda\to\infty} \frac{\langle z_1 z_2 | \hat{H} | z_1 z_2 \rangle}{\langle z_1 z_2 | z_1 z_2 \rangle} \tag{4.5}$$

using in each case the change of variables given in (3.10) and (3.22). The parameter λ is $1/\hbar$ for W_2 and N for SU(3).

In (4.4) $\chi = (N-1)V$ is the interaction parameter and it is held constant as $N \to \infty$; the single particle energies are $\epsilon_0 = -1$, $\epsilon_1 = 0$ and $\epsilon_2 = 1$. The SU(3) classical Hamiltonian represents the time-dependent Hartree–Fock [39] approximation to the quantum fermion dynamics (4.2).

We have computed the projections and Poincaré sections of the associated Husimi distribution for the eigenfunctions of these two models using the equations of sections 3.1 and 3.2; in the case of SU(3) we have diagonalised the Hamiltonian for $\chi = 10$ and $N = 80$, which corresponds to a basis of dimension 861. For the W_2 Nelson potential we take $\mu = 0.1$, $\hbar = 0.01$ and diagonalised on a truncated basis of dimension 806. In both cases the (++) parity subspace was considered.

The aim of this section is to provide some examples of the classical–quantum correspondence between stationary states and classical invariant objects for these two Hamiltonians. For the values of μ and χ we have chosen, both Hamiltonians present, from the classical point of view, a mixed phase space structure with regular and chaotic trajectories forming an intricate mixture of stable and unstable trajectories. A very detailed study of the eigenfunctions of the SU(3) [41] and Nelson [42] Hamiltonians and their correspondence with classical structures has been completed and will be published separately.

In order to associate a definite classical trajectory with a given eigenstate we locate the maximum of the four-dimensional distribution and propagate a classical trajectory from it as an initial condition. This procedure allows a one-to-one association of a wavefunction with a single classical trajectory, which can be said to 'dominate' the quantum state. Secondary maxima can be used to identify other structures.

In figures 1 to 3 we show some selected wavefunctions of the SU(3) model. We have chosen to display the distributions as scatter plots with the density of points proportional to their value; this method emphasises the gross features of the distribution. The projection is plotted on a triangle in accordance to the boundaries established by (3.24).

Figure 1 displays the eigenstates associated with a periodic trajectory. It belongs to a classical family contained in the invariant plane $I_2 = 0$. In the triangles we show the

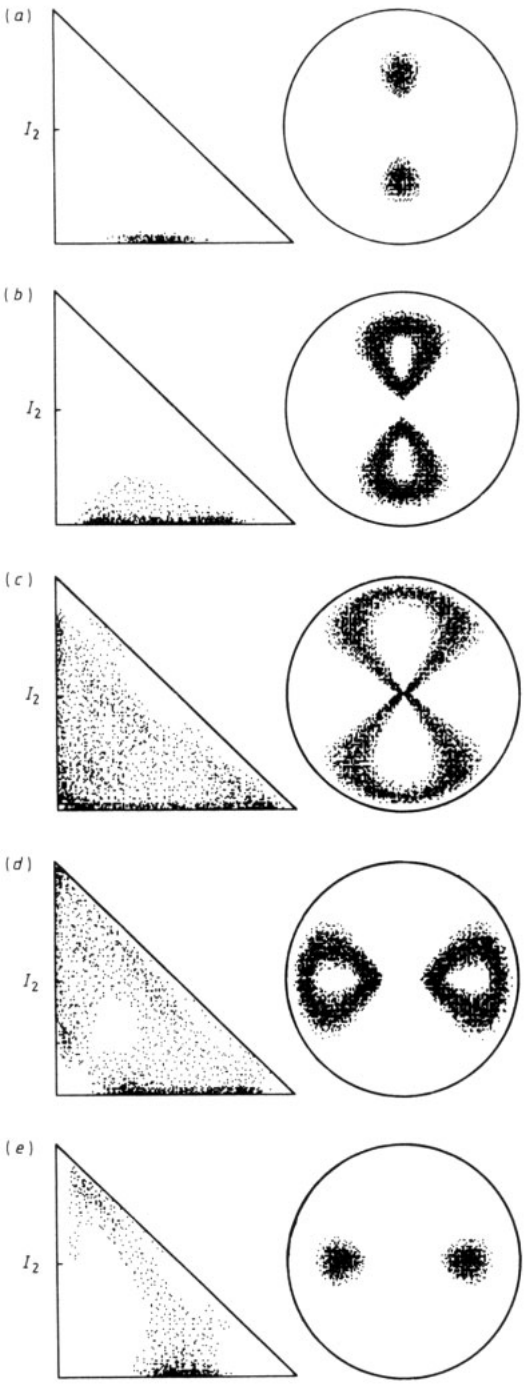

Figure 1. Some SU(3) eigenstates associated with the periodic family of trajectories at $I_2 = 0$. The action variables I_i have the range $0 \leq I_i \leq 1$, while the variables appearing in the circles are I_1 (radius) and θ_1 (angle) (these remarks are valid for all the figures of the paper). The triangles show the wavefunctions and the circles their Poincaré section in the plane $I_2 = 0$. For the energies of eigenstates (*c*), (*d*) and (*e*) the associated classical trajectory is unstable.

projections in the $I_1 I_2$ plane of the Husimi distribution, while the circles on the right display the quantum Poincaré sections obtained in the polar variables I_1, θ_1 with the plane of section $I_2 = 0$. In the Poincaré section the trajectory does not show up as a set of fixed points because the plane of section is chosen so as to contain the entire trajectory.

Classically, this is a very simple family which exists in the invariant plane $I_2 = 0$ because of symmetry. Wavefunctions corresponding to this family are characterised by a strong concentration of probability in the $I_2 = 0$ axis. The family is stable at the beginning (low energies, figure 1(*a*) and 1(*b*)) and then becomes unstable, a fact reflected in the wavefunction by the spreading from the $I_2 = 0$ axis (figures 1(*c*) to 1(*e*)): the wavefunctions are still strongly concentrated on the $I_2 = 0$ axis but now there is a considerable probability out of it. States (*a*) and (*e*) are the first and last states of a large number of states associated with this family. This set of non-statistical wavefunctions concentrated on unstable periodic trajectories even in regions of phase space where the system has large chaotic regions are to be compared with the ones observed by Heller [10] in the chaotic stadium billiard. The states that show such concentration are very regularly spaced at energies given closely by a Bohr–Sommerfeld rule. The striking feature is that both the large amplitudes and the approximate quantisation persist long after the classical family has become unstable. A detailed account of this behaviour is in progress and will be presented elsewhere. We have found at least two other families of wavefunctions associated with periodic trajectories lying on the invariant planes $I_1 = 0$ and $1 - I_1 - I_2 = 0$.

In figure 2(*a*) and 2(*b*) we show two wavefunctions associated with tori. In the upper circle of each figure we plot the quantum Poincaré section in the polar variables I_1, θ_1. The plane of section is indicated by a dotted line in the corresponding triangle. In the bottom part of each figure we show the projection and section for the classical trajectory dominating the wavefunction. An interesting feature of these sections is the appearance of two separate tori in the wavefunctions, as opposed to only one in the classical counterpart. Of course the symmetric classical torus also exists and the observed quantum effect is a coupling of these two Bohr-quantised classical tori due to tunnelling. The calculation of tunnelling probabilities between invariant structures in the case of generic non-integrable Hamiltonians remains as a challenging and important theoretical problem.

Figure 3 is similar to figure 2 but for two chaotic wavefunctions. The associated trajectories fill a three-dimensional volume in phase space as can be seen in the classical section. The comparison of the quantum and classical projections shows that the chaotic trajectory accounts for the main features of the wavefunction. In figure 4 we show for the energy of the wavefunction of figure 3(*b*) the accessible region in the section allowed by energy conservation. Clearly the wavefunction occupies most of the available phase space. The overall pattern is very similar, except for a small non-occupied region observed in the quantum and classical sections of figure 3(*b*) close to the origin. Numerical experiments indicate that this localisation is due to a partial barrier (cantorus) that restrict the spreading of the wavefunction over the entire accessible energy shell. In fact, if we follow the classical trajectory of figure 3(*b*) for longer times, the motion finally enters the non-occupied region.

For the Nelson potential, features concerning periodic trajectories, tori and chaotic regions are quite similar. A simple family of periodic trajectories also exists because of symmetry in the $x = 0$ plane. The period-doubling and in general the n-tupling bifurcations of this family has been extensively studied in [37], which also starts as

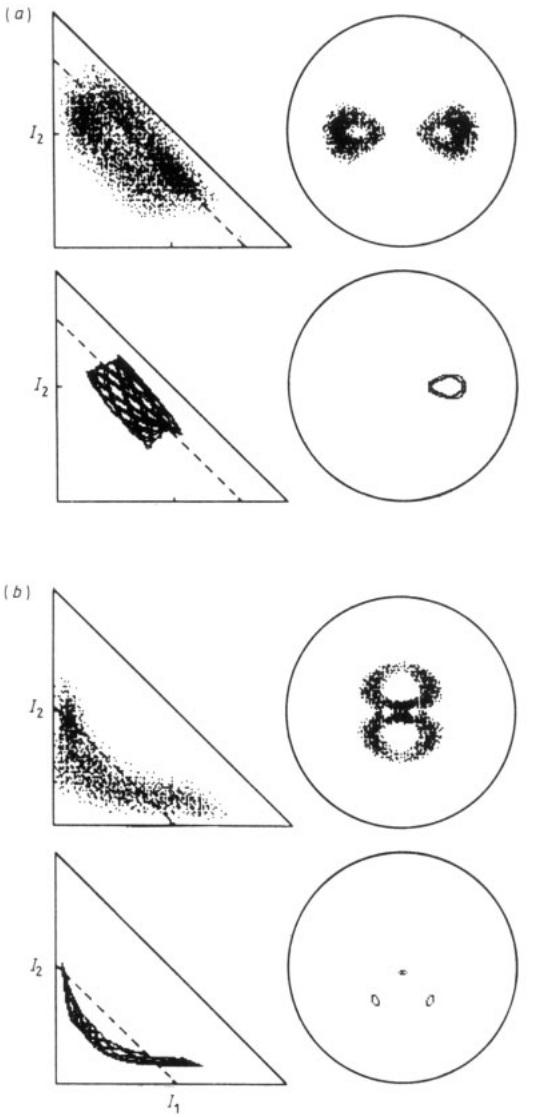

Figure 2. Two SU(3) eigenstates associated with tori. The broken line indicates the plane employed for the section shown in the circles. The quantum distributions and classical dominant trajectories are shown in the upper and lower part of each figure, respectively. Both eigenfunctions present a tunnelling effect between tori.

a stable trajectory, becoming unstable at a period doubling at higher energies. Many states heavily scarred by this family have been found up to energies well into the unstable region. The tori have been studied at low energies in [42].

In figure 5 we show a wavefunction of the Nelson potential that presents a peculiar behaviour as it is dominated by two different periodic trajectories belonging to different families.

The projection of the Husimi distribution in figure 5(*a*) shows two distinct structures that we have labelled A and B. The projection of the classical trajectories that start from the maxima of each of these structures are also displayed and turn out to be

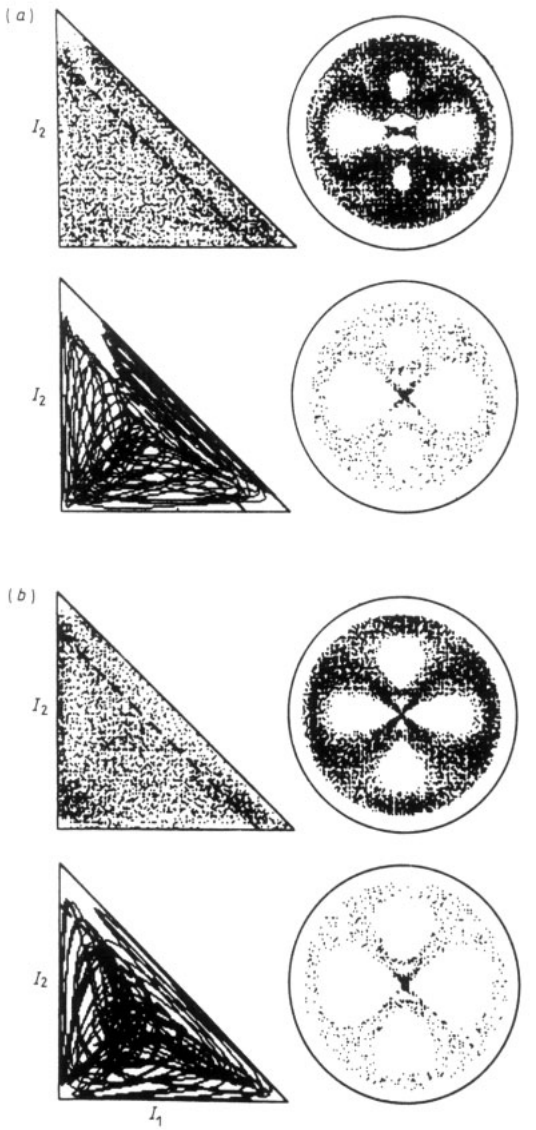

Figure 3. Two SU(3) eigenstates associated with a chaotic region. The classical and quantum Poincaré sections fill three-dimensional volumes. See figure 2 for details.

periodic (the classical projection of the A-structure appears as a single dot in the I_1I_2 plane). The Poincaré section (both classical and quantum) shown in figure 5(*b*) was done at $I_2 = 8$ (dotted line in figure 5(*a*)) and shows the A structure as a central peak and the structure B as four smaller peaks. The intersections of the classical trajectories with that plane of section are indicated by crosses. In both cases we were able to identify these periodic orbits with the families studied in [37]: trajectory A belongs to the vertical family and B is a member of the *I* family at low energy. the reader is referred to [37] for more details on the organisation of the classical trajectories.

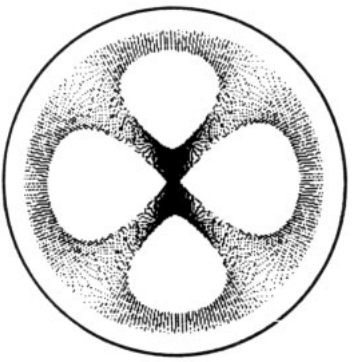

Figure 4. The available classical phase space corresponding to the section of figure 3(*b*). The small difference near the centre of the section between this figure and figures 3(*a*) and 3(*b*) is interpreted in the text as due to a broken torus.

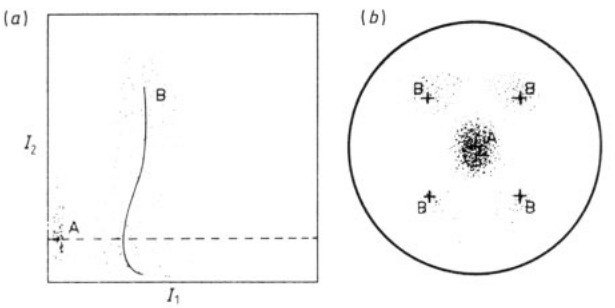

Figure 5. Nelson wavefunction showing the presence of two periodic trajectories *A* and *B*. Part (*a*) displays (superimposed) the quantum (scatter dots) and classical (continuous lines) projections. The periodic orbit A appears as a single dot in these variables. The quantum and classical sections (scatter dots and crosses respectively), made through the plane indicated by a broken line on part (*a*), are shown on (*b*).

5. Conclusion

The aim of this paper has been to explore and develop the generalised Husimi distribution as a tool for the phase space representation of quantum mechanics. We have focused our attention upon conservative systems with two freedoms, which are generically non-integrable. The methods are however very general and are just based on the existence of an underlying group structure and associated coherent states for the transition to the classical limit.

The parallel treatment of the well known case of W_2 and the less known case of SU(3) emphasises that the methods are readily applicable to many situations where a group structure is apparent. The main limitation will be of course the dimension of the phase space as numerical difficulties increase very rapidly with the number of degrees of freedom.

The study of the four dimensional distributions is made comprehensible and easily accessible to computation using their projections and Poincaré sections. We find that the action–angle variables for the distributions are the most appropriate for a comparison of quantum and classical results. In particular, the projections give a smoothed version

of the square of the wavefunction and the smoothing depends on the particular group.

In the two systems that we studied we have found that the gross features of most wavefunctions are explained by a single trajectory, propagated classically from the maximum of the distribution. In the integrable regions this trajectory is, as expected, on a torus, but in the chaotic regions we find many wavefunctions strongly scarred by a single unstable periodic orbit.

Exceptionally we find, as in figure 5, that a wavefunction is made up of two (or more) objects of similar magnitude. We have also found evidence for the existence of cantori which limit the regions of phase space where the chaotic wavefunctions spread. This is an important question which deserves a more thorough investigation. The whole picture is, of course, much more complicated and a study of the distributions at very small amplitude should reveal the presence of other phase space structures. However, the details will be smeared unless much lower values of $\hbar$ (or $1/N$) can be computationally achieved.

Acknowledgments

The work presented in this paper owes an essential part to innumerable discussions with M Baranger. His wisdom and encouragement are gratefully acknowledged. We are also grateful to A Pages for numerical calculations on the Nelson potential.

References

[1] Berry M V 1983 *Chaotic Behavior of Deterministic Systems* (Amsterdam: North-Holland) p 171
[2] Pechukas P 1983 *Phys. Rev. Lett.* **51** 943
[3] Berry M V 1981 *Ann. Phys., NY* **131** 163
Berry M V and Tabor M 1977 *Proc. R. Soc.* A **356** 375
Berry M V 1985 *Proc. R. Soc.* A **400** 229
[4] Bohigas O, Giannoni M J and Schmit C 1984 *Phys. Rev. Lett.* **52** 1
[5] Gutzwiller M C 1982 *Physica* D **5** 183
[6] Berry M V 1985 *Proc. R. Soc.* A **400** 209
[7] Hannay J H and Ozorio de Almeida A M 1984 *J. Phys. A: Math. Gen.* **17** 3429
[8] Balazs N L and Voros A 1986 *Phys. Rep.* **43** 109
[9] Wintgen D 1987 *Phys. Rev. Lett.* **58** 1589
[10] Heller E J 1984 *Phys. Rev. Lett.* **53** 1515
[11] O'Connor P W and Heller E J 1988 *Phys. Rev. Lett.* **61** 2288
[12] Brown R C and Wyatt R E 1986 *Phys. Rev. Lett.* **57** 1
[13] Geisel T, Radons G and Rubner J 1986 *Phys. Rev. Lett.* **57** 2883
[14] Gibson L L, Schatz G C, Ratner M A and Davis M J 1987 *J. Chem. Phys.* **86** 3263
[15] Davis M J 1988 *J. Phys. Chem.* **92** 3124
[16] Gutzwiller M C 1971 *J. Math. Phys.* **12** 343
[17] Bogomolny E B 1988 *Physica* D **31** 169
[18] Berry M V 1989 *Proc. R. Soc.* A **423** 219
[19] Ozorio de Almeida A M 1989 *Nonlinearity* **2** 519
[20] Robnik M 1989 *Preprint* Institute for Theoretical Physics, University of California, Santa Barbara
[21] Yaffe L G 1982 *Rev. Mod. Phys.* **54** 407
[22] Perelomov A 1986 *Generalized Coherent States and their Applications* (New York: Springer)
[23] Husimi K 1940 *Proc. Phys. Math. Soc. Japan* **22** 264
[24] Wigner E 1932 *Phys. Rev.* **40** 749
[25] Balazs N L and Jennings B K 1984 *Phys. Rep.* **104** 347
Hillery M, O'Connel R F, Scully M O and Wigner E P 1984 *Phys. Rep.* **106** 121
[26] Takahashi K 1986 *J. Phys. Soc. Japan* **55** 762

[27] Kurchan J, Leboeuf P and Saraceno M 1989 *Phys. Rev.* A **40** 6800
[28] Berry M V 1977 *Phil. Trans. R. Soc.* **287** 237
[29] Arnol'd V I 1976 *Méthodes Mathématiques de la Mécanique classique* (Moscow: Mir)
[30] Klauder J R 1967 *J. Math. Phys.* **8** 2392
Mckenna J and Klauder J R 1964 *J. Math. Phys.* **5** 878
Bargmann V 1961 *Commun. Pure App. Math.* **XIV** 187
[31] Kramer P and Saraceno M 1981 *Geometry of the Time Dependent Principle in Quantum Mechanics (Lecture Notes in Physics 140)* (New York: Springer)
[32] Kostant B 1970 *Lectures in Modern Analysis and Applications III (Lecture Notes in Mathematics 170)* ed C T Taam (Berlin: Springer) p 87
Kirillov A A 1976 *Elements of the Theory of Representations* (Berlin: Springer)
[33] Lichtenberg A J and Lieberman M A 1984 *Regular and Stochastic Motion* (New York: Springer)
[34] Hutchinson J S and Wyatt R E 1980 *Chem. Phys. Lett.* **72** 378
[35] Weissman Y and Jortner J 1981 *Phys. Lett.* **A83** 55; 1982 *J. Chem. Phys.* **77** 1486
[36] Moshinsky M 1968 *Group Theory and the Many Body Problem* (New York: Gordon & Breach)
[37] Baranger M and Davies K T R 1987 *Ann. Phys., Paris* **177** 330
[38] Li S Y, Klein A and Dreizler R M 1970 *J. Math. Phys.* **11** 975
[39] Williams R D and Koonin S E 1982 *Nucl. Phys.* **A391** 72
[40] Meredith D C, Koonin S E and Zirnbauer M R 1988 *Phys. Rev.* A **37** 3499
[41] Leboeuf P and Saraceno M 1990 *Phys. Rev.* A at press
Leboeuf P 1989 *PhD Thesis* Universidad de Buenos Aires (unpublished)
[42] Mahoney J H 1987 *PhD Thesis* MIT (unpublished)